Fish and Shellfish Immunology 84 (2019) 857–864

Contents lists available at ScienceDirect

Fish and Shellfish Immunology

journal homepage: www.elsevier.com/locate/fsi

Full length article

A20 (*tnfaip3*) is a negative feedback regulator of RIG-I-Mediated IFN induction in teleost

Emilie Mérour, Raphaël Jami, Annie Lamoureux, Julie Bernard, Michel Brémont, Stéphane Biacchesi*

VIM, INRA, Université Paris-Saclay, 78350, Jouy-en-Josas, France

ARTICLE INFO

Keywords:
A20
TNFAIP3
RIG-I
Interferon
Teleost

ABSTRACT

Interferon production is tightly regulated in order to prevent excessive immune responses. The RIG-I signaling pathway, which is one of the major pathways inducing the production of interferon, is therefore finely regulated through the participation of different molecules such as A20 (TNFAIP3). A20 is a negative key regulatory factor of the immune response. Although A20 has been identified and actively studied in mammals, nothing is known about its putative function in lower vertebrates. In this study, we sought to define the involvement of fish A20 orthologs in the regulation of RIG-I signaling. We showed that A20 completely blocked the activation of IFN and ISG promoters mediated by RIG-I. Furthermore, A20 expression in fish cells was sufficient to reverse the antiviral state induced by the expression of a constitutively active form of RIG-I, thus allowing the efficient replication of a fish rhabdovirus, the viral hemorrhagic septicemia virus (VHSV). We brought evidence that A20 interrupted RIG-I signaling at the level of TBK1 kinase, a critical point of convergence for many different pathways that activates important transcription factors involved in the expression of many cytokines. Finally, we showed that A20 expression was directly induced by the RIG-I pathway demonstrating that fish A20 acts as a negative feedback regulator of this key pathway for the establishment of an antiviral state.

1. Introduction

The innate immune response against virus infection is characterized by the induction of a rapid non-specific antiviral state in order to block virus replication and spread. This primary immune response involves a large panel of different pattern recognition receptors (PRRs), including TLRs and RIG-I-like receptors (RLRs), able to detect distinct viral molecular patterns, such as nucleic acids and viral proteins, collectively known as pathogen-associated molecular patterns (PAMPs). PRR activation triggers multiple signaling cascades that lead to the induction of type I interferons (IFNs) which establish the antiviral state and stimulate the adaptive immune response [1]. Among the PRRs, RLRs play a key role in sensing viral nucleic acids in the cell cytosol and are essential in the early induction of type I IFN [2]. Upon viral RNA detection, RIG-I-like receptors reconform and interact with the mitochondrial activator of virus signaling (MAVS) protein, also known as IPS-1, VISA or Cardif. This interaction induces the recruitment of numerous adaptor proteins and kinases to activate IRF3/IRF7 and NF-κB transcription factors which then translocate from the cytosol to the nucleus and induce the expression of the type I IFNs and inflammatory cytokines. Both TANK-binding kinase 1 (TBK1) and inhibitor-κB kinase ε (IKKε) protein kinases phosphorylate IRF3/IRF7, although TBK1 seems to be the main kinase involved in IRF3/IRF7 activation [3–5].

Given the critical role of the RIG-I-mediated IFN induction pathway and to avoid extensive tissue damage upon resolution of infection, negative regulatory loops are essential to maintain the immune homeostatic balance and to ensure the proper termination of the antiviral response [6,7]. Among a long list of molecules, the NF-κB dependent gene, A20, also known as tumor necrosis factor alpha-induced protein 3 or TNFAIP3 [8], has emerged as a key player in the termination of tumor necrosis factor (TNF)-induced apoptosis [9], the negative feedback regulation of inflammation mediated by NF-κB [10,11], and the negative control of the IFN pathway by preventing prolonged IRF3 activation and IFN overexpression following viral infection [12,13]. A20 is a cytoplasmic protein of 90 kDa that is expressed in most cell types and with dual catalytic activity. A20 is an ubiquitin-editing protein with a deubiquitinase activity mediated by its ovarian tumor (OTU) domain at the N-terminal and a C-terminal domain characterized by a seven zinc finger (ZF) structure functioning as an E3 ubiquitin ligase. A20 catalyzes the K48-linked ubiquitylation of target proteins through

* Corresponding author.
E-mail address: stephane.biacchesi@inra.fr (S. Biacchesi).

https://doi.org/10.1016/j.fsi.2018.10.082
Received 30 August 2018; Received in revised form 1 October 2018; Accepted 29 October 2018
Available online 30 October 2018
1050-4648/

its C-terminal ZF domain, a signal for proteasomal degradation. In parallel, A20 removes K63-linked ubiquitin chains, which function as docking sites for protein-protein interactions, from its target proteins through its N-terminal OTU domain. The removal of K63-linked ubiquitin chains inactivates the signaling function of the target proteins and facilitates its K48-linked ubiquitylation and degradation [11].

A20 has been demonstrated as an important negative regulator of RIG-I signaling [14]. In response to viral infection, RIG-I-like receptors (RIG-I/MDA5) recognize viral RNA and trigger the downstream cascade through the mitochondrial adaptor MAVS and the E3 ubiquitin ligase TRAF3. TRAF3 mediates K63-linked polyubiquitinations of some TBK1 lysine residues, a post-translational modification required for TBK1 activation by trans-autophosphorylation [15]. As a critical kinase involved in IFN expression, the activity of TBK1 must be tightly regulated [7]. The A20 regulatory complex, including tax1-binding protein 1 (TAX1BP1) and A20 binding inhibitor of NF-κB 1 (ABIN1) in association with A20, antagonizes K63-linked polyubiquitination of TBK1 by disrupting the interaction between TBK1 and TRAF3 [16,17]. However, it is still unclear whether the inhibitory effect on IRF3/IRF7 is direct, through A20 binding to TBK1 and decrease of TBK1 kinase activity, and/or indirect through A20 recruitment to the adaptor molecule TAX1BP1, where it cooperates with ABIN1 to inhibit TBK1 activation [14].

The IFN system is remarkably conserved in vertebrates. In particular, teleost fish possess functional RLR pathway whose induction by viral pathogens leads to the induction of type I interferon. Several groups showed that fish have orthologs of human RLRs, including RIG-I, MDA5 and LGP2, as well as several downstream signaling molecules, such as MAVS, TBK1/IKKε and IRF3/IRF7 [18,19]. To date, almost nothing is known about the fine regulation of the RIG-I-mediated IFN expression [20]. In the present study, we sought to define the involvement of fish A20 orthologs in the regulation of RIG-I signaling. Activation of IFN or ISG promoters by RIG-I was completely inhibited by A20 expression in fish cells. We showed that A20 interrupted RIG-I signaling at the level of TBK1 by physically interacting and co-localizing with this important kinase. Furthermore, fish cells expressing the active form of RIG-I induced an antiviral state that totally blocked replication of a *Piscine Novirhabdovirus*, the viral hemorrhagic septicemia virus (VHSV), an effect that was reversed by co-expression of A20. Finally, we showed that A20 was up-regulated by the RIG-I pathway itself demonstrating that fish A20 acts as a negative feedback regulator of RIG-I-mediated induction of the antiviral state.

2. Methods

2.1. Cells and virus

EPC cells (Epithelioma Papulosum Cyprini from fathead minnow, *Pimephales promelas*; ATCC CRL-2872) were maintained in Glasgow's modified Eagle's medium-HEPES 25 mM medium (Eurobio) supplemented with 10% fetal bovine serum (FBS, Eurobio) and 2 mM L-glutamine. Recombinant viral hemorrhagic septicemia virus expressing tomato red fluorescent protein (rVHSV-Tom) was propagated in monolayer cultures of EPC cells at 15 °C as previously described [21]. Virus titers were determined by plaque assay on EPC cells under an agarose overlay (0.35% in medium supplemented with 2% FBS and 2 mM L-glutamine). At 3–4 days postinfection, cell monolayers were fixed with 10% formol and stained with crystal violet.

2.2. Molecular cloning and sequencing of fathead minnow and salmon A20

Zebrafish (*Danio rerio*) tnfaip3 gene sequence (XM_687830.7) was used as template to screen expressed sequence tags (ESTs) from fathead minnow (*Pimephales promelas*) and salmon (*Salmo salar*) in the public databases (GenBank) using the nucleotide blast search available on the NCBI website. Total RNA from fathead minnow EPC and Atlantic salmon TO cells were extracted using RNeasy kit (QIAGEN) according to the manufacturer's instructions. The RNA was used to generate full-length cDNAs using the SMART RACE cDNA amplification kit (BD Clontech) with universal primers provided by the manufacturer. PCR amplifications were performed using the Advantage 2 PCR kit (BD Clontech) by following the instructions recommended by the manufacturer for the PCR reaction mixture and the amplification conditions and with gene-specific primers (Table S1A) designed from the ESTs sequences found in GenBank. The overall nucleotide identities of the sequences between zebrafish and fathead minnow and zebrafish and salmon were 83% and 73%, respectively. RT-PCR products were purified with QIAquick PCR purification kit (QIAGEN), cloned into the eukaryotic expression vectors pcDNA1.1/Amp (Invitrogen), modified to fused an HA tag at the 5′ end of the gene of interest, and fully sequenced. The Neighbor-joining (NJ) phylogenetic tree of A20 was calculated by MEGA6 software [22] based on a multiple alignment (using ClustalW) of full-length A20 amino-acid sequences from fish and other vertebrates (protein accession numbers Table S2) and a 1000-boostrap was performed.

2.3. Transfection, fluorescence microscopy and luciferase activity assay

EPC cells were plated into 6-well plates at a density of 5×10^6 cells per well 24 h prior to transfection by electroporation (Amaxa Biosystems; Lonza) as previously described [23]. At 24 or 48 h post-transfection, cells were fixed or lysed for further experiments. Plasmids constructs used in the present study were previously described (RIG-I Nter-eGFP, MAVS, eGFP-MAVS, TBK1, 3xFlag-TBK1, PPM1Bb and IRF3ΔCter) [23–25].

For immunofluorescence microscopy, the cell monolayers were fixed with a mixture of alcohol and acetone [1:1 (v/v)] or with 80% methanol, after mitochondria staining using 500 nM of MitoTracker DeepRed FM (Invitrogen) at −20 °C for 15 min. Antigen detection was performed by incubation with mouse anti-Flag M2 (1/200) or rabbit anti-HA mAbs (1/50; Sigma) diluted in 1x PBS containing 0.05% Tween 20 for 45 min at room temperature. Cells were then washed three times, incubated with Alexa Fluor 488-conjugated anti-mouse and Alexa Fluor 594-conjugated anti-rabbit immunoglobulins (Invitrogen) for 45 min at room temperature and washed again. Cell monolayers were then visualized directly with a UV-light microscope (Carl Zeiss) after mounting of the coverslips using Pro-Long Gold antifade reagent with 4', 6-diamidino-2-phenylindole (DAPI) medium (Invitrogen).

For IFN promoter reporter assays, EPC cells (5×10^6 cells per well of 6-well plate) transfected by electroporation with pIFNpro-LUC [25] or pISRE-LUC (Clontech) together with various plasmid DNA constructs. Some experiments were also performed using an optimized version of the pIFNpro-LUC reporter plasmid consisting on the IFN promoter cloned into a pG5-LUC vector (Promega) and named IFNopt. At 24 h post transfection, cell lysates were prepared using 300 µL of cell culture lysis reagent per well according to the manufacturer's instructions (luciferase reporter assay system - Promega). The level of eGFP expression from peGFP or pRIG-I Nter-eGFP [24] was measured from 100 µL of cell lysates on a Tecan infinite M200 Pro reader using an excitation wavelength of 480 nm and an emission wavelength of 510 nm. Luciferase activity was then measured by adding 100 µL of luciferase assay reagent. Values of luciferase activities were normalized to the levels of eGFP fluorescence. The fold-induction was calculated as the ratio of stimulated versus unstimulated (pcDNA alone) samples. All data are representatives of at least three independent experiments.

2.4. Co-immunoprecipitations, protein electrophoresis and Western blot assays

For co-immunoprecipitation assays, transfected cells in 6-well plates were lysed at 48 h post-transfection using 300 µL of lysis buffer (150 mM NaCl, 50 mM Tris/HCl pH = 8, 20 mM EDTA, 0.5% NP-40 and

complete protease inhibitor cocktail (Roche)). Aliquots of 200 µL were then incubated with 1 µg of mouse anti-Flag M2 mAb (Sigma) or rat anti-HA (Roche) and protein A-Sepharose beads (GE Healthcare) were added. After extensive washes in 1X Tris buffer saline [pH = 7.5] containing 0.5% Tween 20, proteins were eluted with 50 µL of loading buffer. Ten µL of samples were then separated by electrophoresis on a 4–12% gradient polyacrylamide bis-Tris gel (NuPAGE Novex bis-Tris; Invitrogen) followed by western-blotting. After electrotransfer onto a polyvinylidene difluoride membrane (Immobilon-P; Millipore), proteins were detected with a mouse anti-Flag M2 mAb (diluted to 1/500), horseradish peroxidase (HRP)-conjugated rat anti-HA mAb (Roche; diluted to 1/500). Immunodetected antigens were visualized with HRP-conjugated goat anti-mouse immunoglobulin G (P.A.R.I.S.; diluted to 1/5000) by using the enhanced chemiluminescence detection system (ECL; Pierce).

2.5. RNA isolation and qRT-PCR analysis

The EPC IFN was produced in EPC cells using a previously described vector [24]. Briefly, EPC cells were transfected with 2 µg of pcDNA1-IFN1 and the cell supernatant was harvested 3 days later and clarified. Fresh EPC cells were either mock-treated or treated with EPC IFN (1/3 dilution of IFN-transfected EPC cell supernatant). In parallel, EPC cells were transfected with either the RIG-I Nter plasmid construct or an empty vector. At 3 h and 24 h post-treatment, total RNA was extracted using RNeasy kit (QIAGEN) and treated with DNAse. Reverse transcription experiment was performed using iScript Advanced cDNA Synthesis Kit (Bio-Rad), according to the manufacturer's instructions. Gene expression was measured by real time PCR with a CFX Connect Real-Time PCR Detection System (Bio-Rad) using iTaq Universal SYBR green Supermix (Bio-Rad). Each sample is composed of 5 µL primers (500 nM each), 5 µL cDNA (diluted 1/10), and 10 µL PCR Mastermix. Samples were first incubated at 95 °C for 30 s, then subjected to 40 amplification cycles (95 °C for 5 s and 60 °C for 30 s), followed by the melting curve of PCR products from 65 °C to 95 °C with 0.5 °C increment every 5 s. The relative fold induction of the gene of interest, normalized to an endogenous reference (β-actin) and relative to a calibrator (pcDNA-tranfection or mock-infected conditions) was determined using the $2-\Delta\Delta CT$ method [26]. All qPCR primers used in this study are shown in Table S1B.

3. Results

3.1. The mammalian A20 protein has a counterpart in teleost fish

To get insight into the RIG-I pathway regulation in fish, we cloned the full-length A20-related cDNA of cyprinid and salmonid cells. A unique sequence similar to the human A20 was annotated in zebrafish genome on the chromosome 13 (XP_692922). Specific primers were designed from this sequence and used to amplify a cDNA molecule from the EPC cyprinid cells. The EPC A20 cDNA is of 2346 nucleotides (nt) in length and encodes an ORF of 781 amino acids (aa) (GenBank accession no. LT984694). The salmon A20 cDNA was amplified using primers derived from the sequence of tnfaip3 isoform X2 available in GenBank (XM_014179932). Two cDNA were amplified: a small of 2259 nt (GenBank accession no. LT984693) and a large of 2403 nt (GenBank accession no. LT984692) in length encoding a protein of 752 and 800 aa, respectively. The small isoform of salmon A20 amplified in this study was found in GenBank under the accession no. XP_014065911. The small and large salmon isoforms of A20 protein are encoded by paralogous genes located on two different chromosomes, ssa1 and ssa28, respectively. Another salmon isoform, tnfaip3 isoform X1 (XP_014035406), of a larger size (816 aa) is also predicted from the tnfaip3 gene located on the chromosome 28.

Fish A20 proteins present a domain structure similar to that of human A20 (Fig. 1A) including the OTU ubiquitin protease domain and the seven zinc fingers of the E3 ubiquitin ligase domain. The A20 protein is found in fish, mammals and birds (Fig. 1B). A20 proteins share an overall sequence identity of 50% between higher and lower vertebrates (Table S3). Interestingly, the main difference between both salmon paralogs is found in the C-terminal region with several deletions and the loss of one zinc finger (ZF5, Fig. 1A). In the N-terminal region, the OTU domain is highly conserved including residues of the catalytic triad (human: Cys103, His256, Asp70 and fish: Cys107, His258, Asp74). These data suggested that all these sequences constitute true orthologs and thus A20 was conserved throughout the evolution.

3.2. Overexpression of fish A20 inhibits RIG-I-mediated antiviral signaling

To determine whether A20 is involved in the negative regulation of the antiviral response in fish cells, we first tested whether EPC A20 contributes to the inhibition of RIG-I-mediated IFN expression by using a cell-based luciferase reporter system. In all experiments, promoter activities were normalized to the levels of eGFP fluorescence expressed alone or in fusion to RIG-I Nter. In all cases, no significant variation in eGFP expression could be observed (data not shown). As shown in Fig. 2A and B, the expression of a constitutively active form of RIG-I (RIG-I Nter; in which the C-terminal repressor domain maintaining the protein in a latent inactive state was deleted) significantly activated the promoters of IFN1 and interferon-stimulated response element (ISRE) in EPC cells. In contrast, the co-expression of A20 with RIG-I Nter drastically reduced the induction of these two promoters even more efficiently than PPM1Bb, a previously identified inhibitor of this pathway in fish [23]. We next tested whether A20 affected the activation of TBK1. As shown in Fig. 2C, the overexpression of TBK1 activated the promoter of IFN1. The co-expression of A20, as well as PPM1Bb which specifically inhibits TBK1, also significantly suppressed the induction of IFN1 promoter mediated by TBK1, demonstrating a specific and negative effect of A20 on the RIG-I pathway at the level of TBK1 or downstream. Finally, as shown in Fig. 2D, the expression of both isoforms of salmon A20 have the same capacity to inhibit RIG-I Nter induction of IFN1 promoter compared to EPC A20, indicating a conserved function of A20 proteins throughout evolution. Moreover, the loss of one zinc finger (ZF5) in the small isoform of salmon A20 seems to have no effect on the A20 inhibitory function of this IFN-induction pathway.

3.3. A20 repression of the RIG-I Nter-induced antiviral state

To determine whether fish A20 proteins could repress the RIG-I Nter-induced antiviral state, EPC cells were transfected with RIG-I Nter alone or together with EPC A20 or the large isoform of salmon A20. RIG-I Nter was also transfected with the dominant negative form of IRF3 (IRF3ΔCter) which was previously shown to be able to block RIG-I Nter-stimulated expression of endogenous IFN and ISG genes [25]. These transfected cells were then infected with rVHSV-Tom at an MOI of 1 and viral replication was followed by visualizing Tomato red fluorescence protein expression under a UV-visible light microscope (Fig. 3A). In the control condition at 24 h postinfection, EPC cell monolayer was efficiently infected by rVHSV-Tom whereas in RIG-I Nter-expressing cells, virus infection was almost completely prevented. In contrast, in cells that co-expressed either A20 from EPC or from salmon, efficient rVHSV-Tom infection could be observed even in cells expressing high level of RIG-Nter and similarly to that in cells expressing the dominant negative form of IRF3. As shown in Fig. 3B, the EPC cell monolayer that expressed RIG-I Nter was protected against rVHSV-Tom infection, whereas total cytopathic effects were reached in cells co-expressing A20 proteins at day 4 postinfection. This observation was in accordance to the viral titers measured at 48 h post-infection. Indeed, in EPC cells expressing RIG-I Nter alone, the virus titer only reached 1.6×10^4 PFU/mL, but in presence of the A20 proteins the virus titers were 1.1–1.8 $\times 10^7$ PFU/mL and just 10-fold reduced compared to that of the non-transfected control (1.4×10^8 PFU/mL). Taken together,

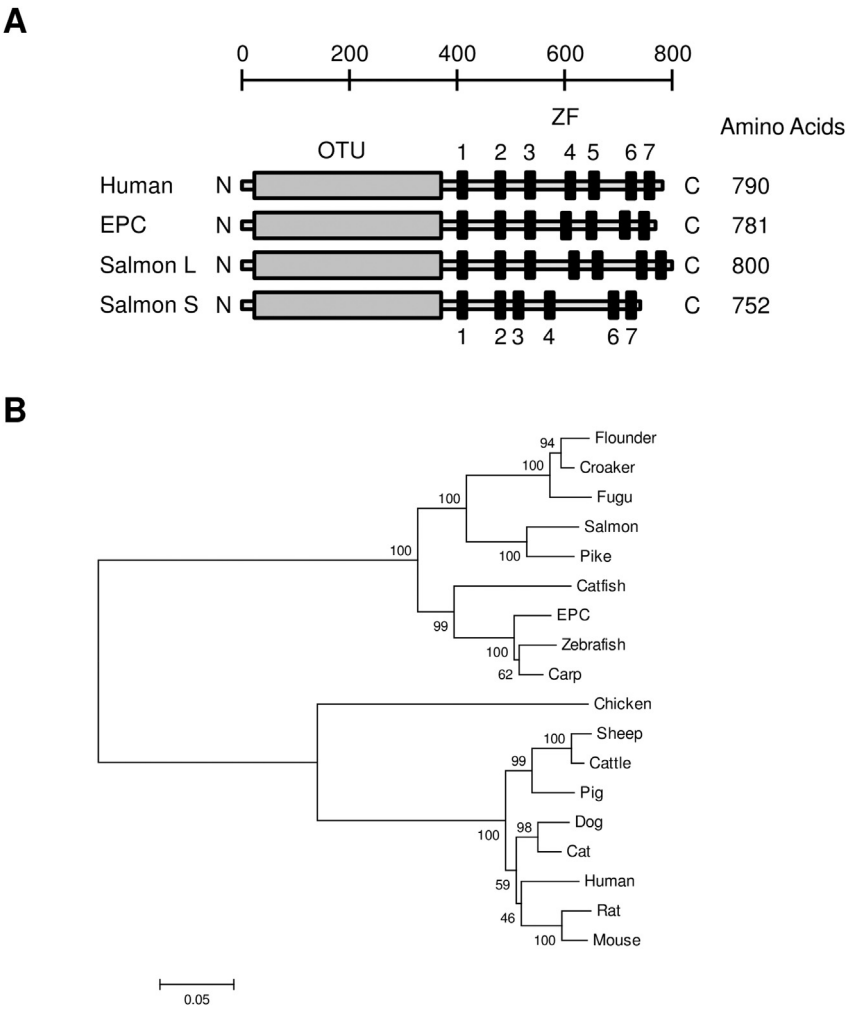

Fig. 1. Conservation of A20 in vertebrates. **A.** Domain structure of fish A20 orthologs compared to human A20. Ovarian tumor (OTU) ubiquitin protease domain and zinc fingers (ZF) E3 ubiquitin ligase domain are depicted in gray and black boxes, respectively. **B.** NJ phylogenetic tree of vertebrate A20. The tree was based on multiple alignments of full-length A20 amino-acid sequences from fish and other vertebrates. Numbers near nodes correspond to percent bootstrap support and the scale represents the number of substitutions per site. The tree is drawn to scale.

these results demonstrate that fish A20 can efficiently block the RIG-I-mediated signaling pathway and down-regulate cellular antiviral response.

3.4. Co-localization and interaction of A20 avec TBK1

Because fish A20 seems to negatively regulate the antiviral signaling at the level of TBK1, we asked whether A20 targets TBK1 by protein-protein interactions. First, the subcellular localization of A20 was studied by immunofluorescence assay in EPC cells expressing A20 alone or together with different actors of the RIG-I pathway. When expressed alone, A20 displayed a diffuse staining in the cell cytoplasm and did not localize in the vicinity of mitochondria (Fig. 4A). In contrast, in RIG-I Nter, MAVS and TBK1 co-transfected cells, A20 presented a punctate perinuclear staining (Fig. 4 B, C and D, respectively). A20 did not co-localize with RIG-I Nter and MAVS. Interestingly, similar punctate perinuclear staining was observed for TBK1. In those structures, A20 was shown to be greatly co-localized with TBK1. In order to confirm the interaction between A20 and TBK1, we performed co-immunoprecipitation experiments. As shown in Fig. 5, a major specific band of approximately 100 kDa was detected for TBK1 in EPC cell lysates for a calculated molecular weight of 87 kDa for the tagged version of TBK1. For A20, only a unique specific band was detected in cell lysates around 100 kDa for a calculated molecular weight of 90 kDa for the tagged version of A20. Both Epitope-tagged proteins reciprocally co-immunoprecipitated in transfected EPC cells demonstrating that TBK1 and A20 interact together.

3.5. A20 expression is enhanced by the activation of RIG-I pathway

Since A20 acts as a negative regulator of the RIG-I-mediated IFN induction, we wondered whether A20 gene expression could be up-regulated by RIG-I signaling activation or by IFN expression. Therefore, we measured A20 gene expression in EPC cells after either the expression of the constitutively active form of RIG-I (RIG-I Nter) or a treatment with IFN (Fig. 6). We first examined IFN expression as a control of IFN paracrine function or as a marker of RIG-I signaling activation (Fig. 6A). As soon as 3 h, a 3 log increase of IFN expression was observed in IFN-treated EPC cells that lasted up to 24 h. In RIG-I Nter expressing EPC cells, IFN expression was induced later and reached a 2 log induction at 24 h. These results indicated that both stimulations were efficient to induce IFN in EPC cells. In contrast, IFN treatment had no effect on the A20 expression whereas activation of RIG-I signaling up-regulated A20 expression by 14-fold at 24 h post-transfection (Fig. 6B). The up-regulation of A20 expression by the RIG-I pathway itself indicates that A20 functions as a negative feedback regulator of RIG-I signaling in fish cells.

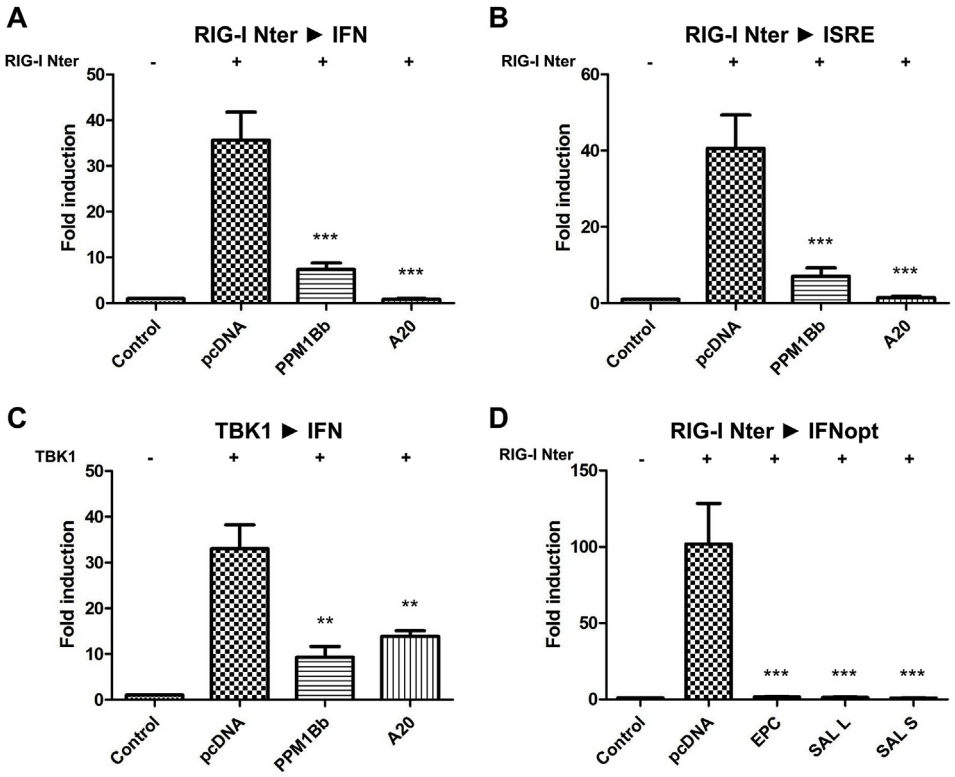

Fig. 2. Overexpression of fish A20 proteins negatively regulates RIG-I pathway. **A** and **B.** Overexpression of EPC A20 reduced RIG-I-induced activation of the IFN1 and ISRE promoters. EPC cells were transfected with the indicated plasmids (1 μg) together with luciferase reporter constructs (1 μg) driven by the promoters of genes encoding IFN1 (A) or ISRE (B), and RIG-I Nter-eGFP as inducer and internal control (1 μg). In cases where RIG-I Nter-eGFP was omitted, peGFP (1 μg) was added as internal control. All transfection mixtures were adjusted with an empty vector (pcDNA) to obtain an equal total quantity of plasmid DNA. Twenty-four hours after transfection, the cells were lysed for luciferase assays. Luciferase activity was measured and normalized to eGFP fluorescence. The fold inductions were calculated as the ratio of stimulated (+RIG-I-Nter) versus unstimulated (Control; - RIG-I-Nter) samples. Means of at least three independent experiments are shown together with the standard errors. For statistical analysis, a comparison between groups was performed with a one-way ANOVA and Tukey's multiple comparison tests using GraphPad Prism (GraphPad, San Diego, CA). Groups that are significantly different are noted ** ($p < 0.01$) or *** ($p < 0.001$). **C.** Overexpression of EPC A20 reduced TBK1-induced activation of the IFN1 promoter. EPC cells were transfected with the indicated plasmids (1 μg) together with a luciferase reporter construct driven by the promoter of IFN1 (1 μg), TBK1 (1 μg) as inducer and peGFP (1 μg) as internal control. Twenty-four hours post transfection, luciferase assays were performed and analyzed as described above. **D.** Fish A20 inhibit RIG-I-mediated IFN expression. EPC cells were transfected with an optimized plasmid construct expressing the luciferase reporter under the control of the IFN1 promoter (IFNopt; 1 μg), and RIG-I Nter-eGFP as inducer and internal control (1 μg) together with DNA plasmids (1 μg) encoding EPC A20 or small (S) and large (L) forms of salmon A20, as indicated. Twenty-four hours post transfection, luciferase assays were performed, and analyzed as described above.

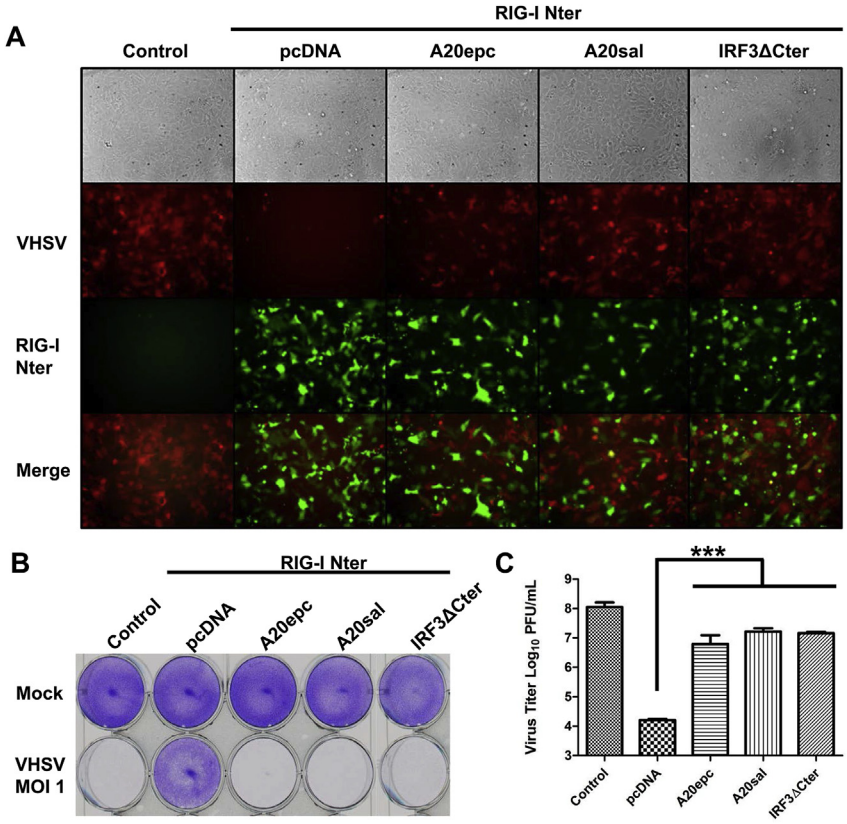

Fig. 3. Overexpression of fish A20 proteins inhibits RIG-I-mediated antiviral response. EPC cells were transfected with the indicated plasmids (1 μg each) together with RIG-I Nter-eGFP as inducer of the antiviral response or mock transfected (control). Twenty-four hours after transfection, cells were infected with rVHSV-Tom, expressing the tomato red fluorescent protein at an MOI of 1 and incubated at 15 °C. Cell monolayers were visualized under a UV-visible light microscope at 24 h postinfection (**A**) and then were stained with crystal violet 4 days postinfection (**B**). The culture supernatants from cells infected with rVHSV-Tom were collected at 48 h postinfection and the viral titer was determined by plaque assay on EPC cells (**C**). Each time point was represented by two independent experiments, and each virus titration was done in duplicate. Means are shown. The standard errors were calculated and the error bars are shown. Asterisks indicate significant difference (***$p < 0.001$) as determined by one-way ANOVA and Tukey's multiple comparison tests.

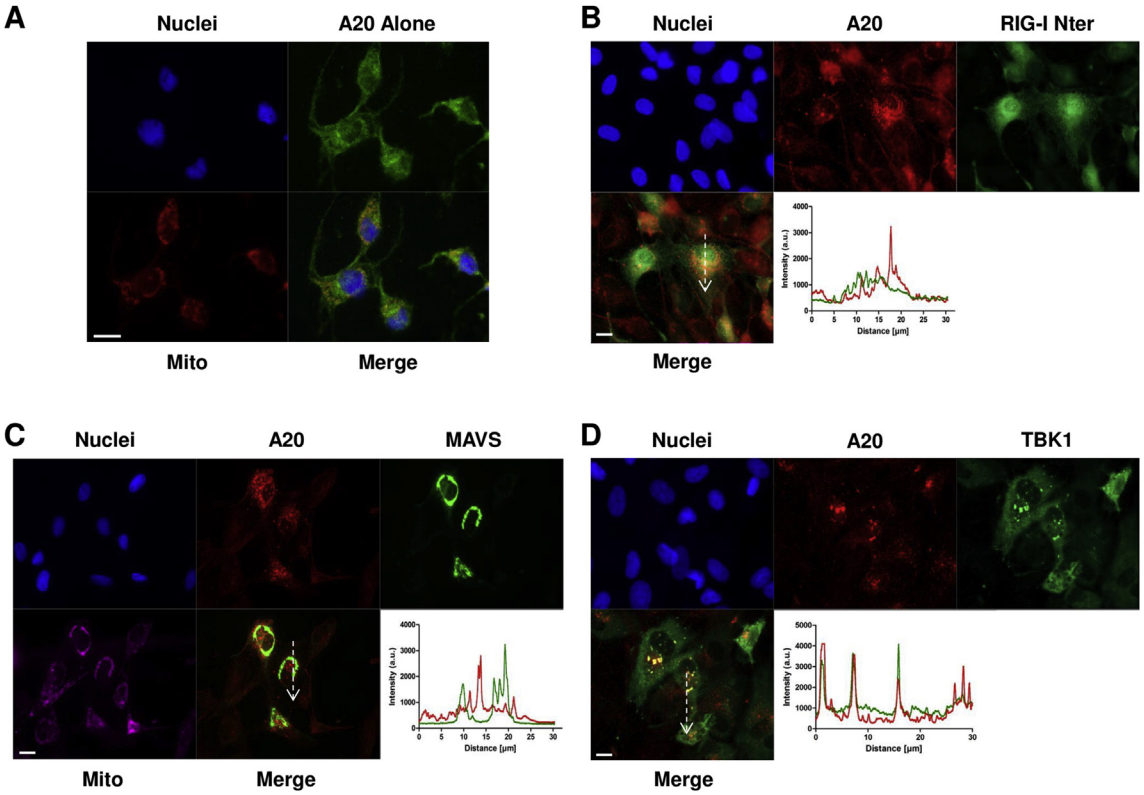

Fig. 4. A20 co-localizes with TBK1. EPC cells were transfected with 1.5 μg of the indicated plasmids alone (**A**) and in combination (**B**, **C** and **D**) for 24 h. Cell mitochondria were then stained with a deep red MitoTracker. After fixation, A20 and TBK1 proteins were detected with anti-HA and anti-Flag mAbs, respectively. RIG-I Nter and MAVS were fused to eGFP and the nuclei were stained by DAPI. For each panel (**B–D**), an intensity line graph is presented showing the intensity of the red color (A20) and the green color (RIG-I Nter, MAVS or TBK1) along the dotted white line in the merge image. Scale bars, 10 μm.

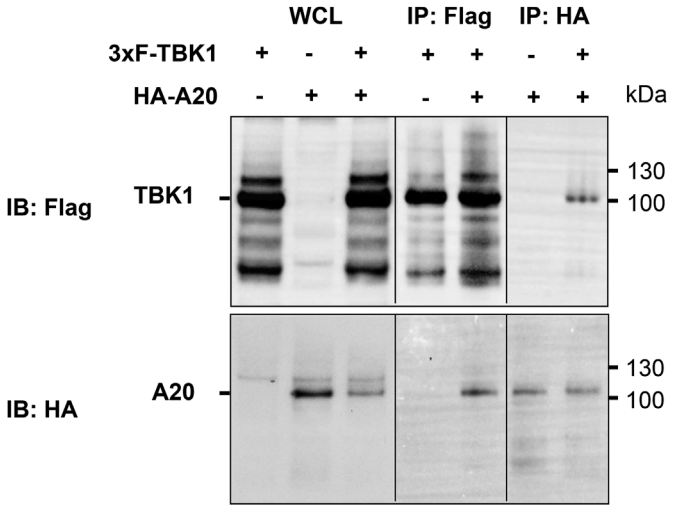

Fig. 5. A20 interacts withTBK1. Epitope-tagged A20 and TBK1 proteins interact with each other in EPC cells. EPC cells were co-transfected with 1.5 μg of the indicated plasmids. At 48 h post transfection, the lysates were immunoprecipitated (IP) with anti-HA or anti-Flag as indicated, followed by immunoblotting (IB) analysis with anti-HA or anti-Flag. WCL corresponds to the expression of exogenous proteins in whole-cell lysates.

4. Discussion

The results of the present study demonstrate that fish A20 proteins were true orthologs of mammalian A20. Fish A20 proteins efficiently block RIG-I signaling. Interestingly, both salmon paralogs (small and large paralogs) display the same efficacy to inhibit the induction of the IFN promoter, despite of the partial loss of a zinc finger in the C-terminal domain of the small paralog (Fig. 1A). Nevertheless, this deletion only affects the zinc finger 5 (ZF5) of the small paralog which is not the main ZF involved in the inhibition of RIG-I signaling. Indeed, in a previous study, deletions mutants of human A20 indicated that the C-terminal region, and more particularly the ZF7, was required for the complete inhibition of RIG-I signaling [12]. Expression of A20 completely prevents the induction of the antiviral state by the active form of RIG-I (RIG-I Nter), restoring VHSV replication in RIG-I Nter expressing cells. The blockage of the IFN-induction cascade by A20 takes place at the level of TBK1, a critical point of convergence for many different PRR pathways that activates IRF3/IRF7. Finally, A20 expression was significantly up-regulated by the activation of the RIG-I pathway and not by IFN stimulation. All these results indicate that fish A20, as well as mammalian A20 orthologs, functions as a negative feedback loop regulator of RIG-I-mediated induction of the antiviral state.

In a previous study, Wang and colleagues reported that mammalian A20 completely block the RIG-I Nter-induced IFN promoter activation but not that induced by TBK1 or IKKε [27]. Similarly, Lin and colleagues observed that A20 only minimally reduced TBK1- or IKKε-induced ISRE promoter activity, suggesting that the level of A20 inhibition was upstream of TBK1/IKKε kinases [12]. In contrast, Saitoh and colleagues demonstrated that A20 interrupted RIG-I signaling by physically interacting with TBK1 and IKKε kinases, thereby blocking phosphorylation and subsequent dimerization of IRF3 [13]. In the present study, we also showed that fish A20 completely inhibited RIG-I Nter-mediated IFN and ISRE promoter activation (Fig. 2A and B, respectively). Fish A20 partially blocked the activation of IFN promoter by TBK1 overexpression (Fig. 2C), but at least as well as PPM1B which targets TBK1 as one of its substrates [23]. We also found that A20 and TBK1 are components of the same protein complex by co-immunoprecipitation (Fig. 5). Moreover, upon RIG-I signaling activation by overexpression of

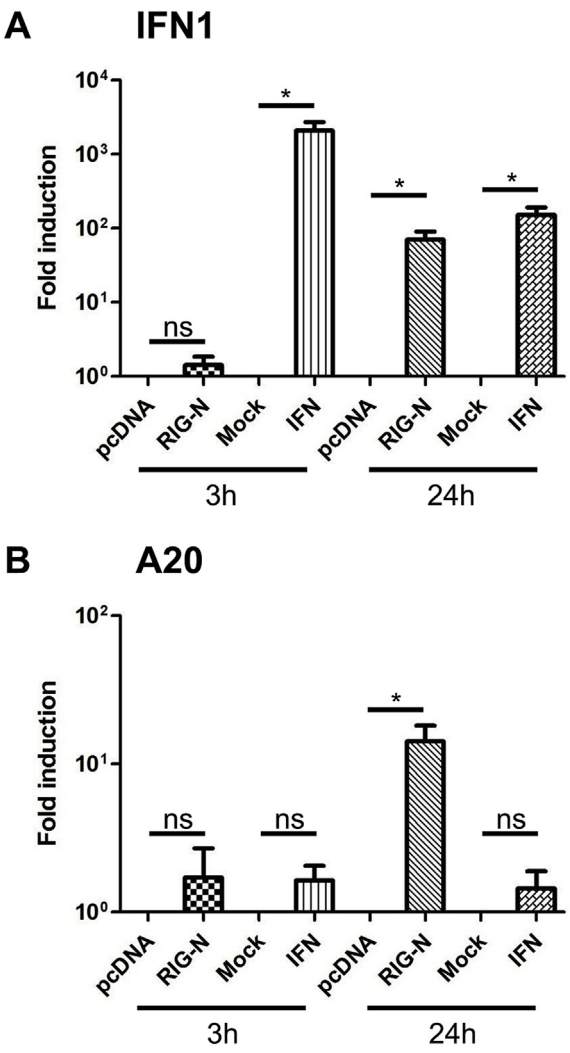

Fig. 6. A20 is directly induced by RIG-I signaling. EPC cells were either transfected with 1 μg of RIG-I Nter plasmid construct or an empty vector (pcDNA) as a control. In parallel, EPC cells were either mock-treated (Mock) or treated with EPC IFN. At 3 h and 24 h posttransfection or posttreatment, total RNA were extracted and RT performed. Quantitative real-time PCR was conducted using primers targeting IFN1 (**A**) and A20 (**B**). The β-actin gene was used as an internal control to normalize the cDNA template and for real-time PCR calculations. The standard deviations for triplicate experiments are shown. Asterisks indicate significant difference (*$p < 0.01$) as determined by a one-way ANOVA and Tukey's multiple comparison tests using GraphPad Prism (GraphPad, San Diego, CA). ns, not significant.

either RIG-I Nter, MAVS or TBK1, A20 has been shown to relocalize to vesicular structures around the nucleus where it strongly co-localize with TBK1 (Fig. 4). These results suggest that A20 inhibits RIG-I signaling at the level of TBK1. Additional experiments will be necessary to dissect the protein complex in which TBK1 and A20 interact together and evaluate whether fish A20 also requires TAX1BP1 and ABIN1 in order to inhibit RIG-I signaling at the level of TBK1/IKKε, as described in mammals [16,17]. TAX1BP1 and ABIN1 are relatively well conserved in vertebrates and are annotated in several fish genome. Furthermore, in catfish gills infected by columnaris bacteria (*Flavobacterium columnare*), it has been suggested that the up-regulation of TAX1BP1 was involved in the suppression of NF-κB activation and in the inhibition of inflammatory signaling [28].

A20 was originally described as a TNFα-inducible gene whose expression constitutes a negative feedback loop for NF-κB signaling, aiming at containing inflammation [29,30]. The NF-κB inhibitory function of A20 was formally established in response to multiple inflammatory stimuli, including TNFα, IL-1b, LPS and H_2O_2. A20 is also essential for the termination of TLR induced NF-κB activation in macrophages [31]. The inhibition of both IRF- and NF-κB-dependent pathways underscores the key role played by A20 as a negative feedback regulator of immune response signaling. In the present study, fish A20 were showed to be important negative regulators of RIG-I signaling. It will be of interest to determinate whether fish A20 are also key regulator components of the TNF-α- and TLR-signaling. Recent publications highlight important functions of TNF-α as a key cytokine in the activation of the immune system [32,33] and as a mediator of behavioral fever upon viral infection in fish [34]. Furthermore, new data were provided on how fish viruses could alter TNF-α signaling and even hijack it to their own benefit. Rakus and colleagues demonstrated that carp exhibit behavioral fever in response to virus infection by transiently migrating in warmer temperature water and that change of temperature increase their survival. In order to counteract this behavior, cyprinid herpesvirus 3 encodes a soluble decoy receptor for TNF-α which delays the manifestation of behavioral fever in infected carp and thus promotes virus replication [34]. In another study, Espin-Palazon and colleagues provided new insights on TNF-α deleterious effect on zebrafish survival to spring viremia of carp virus infection (SVCV) [35]. Indeed, the depletion of TNF-α or its receptor (TNFR2) increase zebrafish larvae survival upon SVCV infection. Although TNF-α expression levels has no effect on the interferon response and SVCV replication in zebrafish, TNF-α blocks the host autophagic response, which is required for viral clearance. In this zebrafish model, TNF-α inhibits autophagy probably through the activation of NF-κB [36], whose activation is tightly regulated by A20.

In conclusion, this work provides the first demonstration that A20 protein function is conserved in vertebrates as a negative regulator of the cellular antiviral response in order to maintain immune homeostasis.

Author contributions

SB conceived and designed the experiments. EM, RJ, AL, JB and SB performed the experiments. EM, RJ and SB analyzed the data. MB provided financial support, thorough discussions and critical manuscript reading. SB wrote the manuscript.

Competing financial interests

The authors declare no competing financial interests.

Acknowledgments

We thank Jean Millet for critical reading of the manuscript.

Appendix A. Supplementary data

Supplementary data to this article can be found online at https://doi.org/10.1016/j.fsi.2018.10.082.

References

[1] J. Chow, K.M. Franz, J.C. Kagan, PRRs are watching you: localization of innate sensing and signaling regulators, Virology 479–480 (2015) 104–109.
[2] M. Yoneyama, et al., Viral RNA detection by RIG-I-like receptors, Curr. Opin. Immunol. 32 (2015) 48–53.
[3] K.A. Fitzgerald, et al., IKKepsilon and TBK1 are essential components of the IRF3 signaling pathway, Nat. Immunol. 4 (5) (2003) 491–496.
[4] S.M. McWhirter, et al., IFN-regulatory factor 3-dependent gene expression is defective in Tbk1-deficient mouse embryonic fibroblasts, Proc. Natl. Acad. Sci. U. S. A. 101 (1) (2004) 233–238.
[5] S. Sharma, et al., Triggering the interferon antiviral response through an IKK-related pathway, Science 300 (5622) (2003) 1148–1151.
[6] Y.K. Chan, M.U. Gack, RIG-I-like receptor regulation in virus infection and

immunity, Curr. Opin. Virol. 12 (2015) 7–14.
[7] W. Zhao, Negative regulation of TBK1-mediated antiviral immunity, FEBS Lett. 587 (6) (2013) 542–548.
[8] A. Krikos, C.D. Laherty, V.M. Dixit, Transcriptional activation of the tumor necrosis factor alpha-inducible zinc finger protein, A20, is mediated by kappa B elements, J. Biol. Chem. 267 (25) (1992) 17971–17976.
[9] A.W. Opipari Jr.et al., The A20 zinc finger protein protects cells from tumor necrosis factor cytotoxicity, J. Biol. Chem. 267 (18) (1992) 12424–12427.
[10] N. Shembade, A. Ma, E.W. Harhaj, Inhibition of NF-kappaB signaling by A20 through disruption of ubiquitin enzyme complexes, Science 327 (5969) (2010) 1135–1139.
[11] I.E. Wertz, et al., De-ubiquitination and ubiquitin ligase domains of A20 downregulate NF-kappaB signalling, Nature 430 (7000) (2004) 694–699.
[12] R. Lin, et al., Negative regulation of the retinoic acid-inducible gene I-induced antiviral state by the ubiquitin-editing protein A20, J. Biol. Chem. 281 (4) (2006) 2095–2103.
[13] T. Saitoh, et al., A20 is a negative regulator of IFN regulatory factor 3 signaling, J. Immunol. 174 (3) (2005) 1507–1512.
[14] M. Arguello, et al., Anti-viral tetris: modulation of the innate anti-viral immune response by A20, Adv. Exp. Med. Biol. 809 (2014) 49–64.
[15] A. Outlioua, M. Pourcelot, D. Arnoult, The role of optineurin in antiviral type I interferon production, Front. Immunol. 9 (2018) 853.
[16] L. Gao, et al., ABIN1 protein cooperates with TAX1BP1 and A20 proteins to inhibit antiviral signaling, J. Biol. Chem. 286 (42) (2011) 36592–36602.
[17] K. Parvatiyar, G.N. Barber, E.W. Harhaj, TAX1BP1 and A20 inhibit antiviral signaling by targeting TBK1-IKKi kinases, J. Biol. Chem. 285 (20) (2010) 14999–15009.
[18] S.N. Chen, P.F. Zou, P. Nie, Retinoic acid-inducible gene I (RIG-I)-like receptors (RLRs) in fish: current knowledge and future perspectives, Immunology 151 (1) (2017) 16–25.
[19] S. Poynter, et al., Sensors of infection: viral nucleic acid PRRs in fish, Biology 4 (3) (2015) 460–493.
[20] A. Rebl, T. Goldammer, Under control: the innate immunity of fish from the inhibitors' perspective, Fish Shellfish Immunol. 77 (2018) 328–349.
[21] S. Biacchesi, et al., Limited interference at the early stage of infection between two recombinant novirhabdoviruses: viral hemorrhagic septicemia virus and infectious hematopoietic necrosis virus, J. Virol. 84 (19) (2010) 10038–10050.
[22] K. Tamura, et al., MEGA6: molecular evolutionary genetics analysis version 6.0, Mol. Biol. Evol. 30 (12) (2013) 2725–2729.
[23] S. Biacchesi, et al., NV proteins of fish Novirhabdovirus recruit cellular PPM1Bb protein phosphatase and antagonize RIG-I-mediated IFN induction, Sci. Rep. 7 (2017) 44025.
[24] S. Biacchesi, et al., Mitochondrial antiviral signaling protein plays a major role in induction of the fish innate immune response against RNA and DNA viruses, J. Virol. 83 (16) (2009) 7815–7827.
[25] S. Biacchesi, et al., Both STING and MAVS fish orthologs contribute to the induction of interferon mediated by RIG-I, PLoS One 7 (10) (2012) e47737.
[26] K.J. Livak, T.D. Schmittgen, Analysis of relative gene expression data using real-time quantitative PCR and the 2(-Delta Delta C(T)) Method, Methods 25 (4) (2001) 402–408.
[27] Y.Y. Wang, et al., A20 is a potent inhibitor of TLR3- and Sendai virus-induced activation of NF-kappaB and ISRE and IFN-beta promoter, FEBS Lett. 576 (1–2) (2004) 86–90.
[28] F. Sun, et al., Transcriptomic signatures of attachment, NF-kappaB suppression and IFN stimulation in the catfish gill following columnaris bacterial infection, Dev. Comp. Immunol. 38 (1) (2012) 169–180.
[29] J.T. Cooper, et al., A20 blocks endothelial cell activation through a NF-kappaB-dependent mechanism, J. Biol. Chem. 271 (30) (1996) 18068–18073.
[30] M. Jaattela, et al., A20 zinc finger protein inhibits TNF and IL-1 signaling, J. Immunol. 156 (3) (1996) 1166–1173.
[31] D.L. Boone, et al., The ubiquitin-modifying enzyme A20 is required for termination of Toll-like receptor responses, Nat. Immunol. 5 (10) (2004) 1052–1060.
[32] S. Hong, et al., Two types of TNF-alpha exist in teleost fish: phylogeny, expression, and bioactivity analysis of type-II TNF-alpha3 in rainbow trout Oncorhynchus mykiss, J. Immunol. 191 (12) (2013) 5959–5972.
[33] F.J. Roca, et al., Evolution of the inflammatory response in vertebrates: fish TNF-alpha is a powerful activator of endothelial cells but hardly activates phagocytes, J. Immunol. 181 (7) (2008) 5071–5081.
[34] K. Rakus, et al., Conserved fever pathways across vertebrates: a herpesvirus expressed decoy TNF-alpha receptor delays behavioral fever in fish, Cell Host Microbe 21 (2) (2017) 244–253.
[35] R. Espin-Palazon, et al., TNFalpha impairs rhabdoviral clearance by inhibiting the host autophagic antiviral response, PLoS Pathog. 12 (6) (2016) e1005699.
[36] M. Djavaheri-Mergny, et al., NF-kappaB activation represses tumor necrosis factor-alpha-induced autophagy, J. Biol. Chem. 281 (41) (2006) 30373–30382.